



**HAL**  
open science

## Cosolvents in Self-Emulsifying Drug Delivery Systems (SEDDS): Do They Really Solve Our Solubility Problems?

Arne Matteo Jörgensen, Julian David Friedl, Richard Wibel, Joseph Chamieh, Hervé Cottet, Andreas Bernkop-Schnürch

► **To cite this version:**

Arne Matteo Jörgensen, Julian David Friedl, Richard Wibel, Joseph Chamieh, Hervé Cottet, et al.. Cosolvents in Self-Emulsifying Drug Delivery Systems (SEDDS): Do They Really Solve Our Solubility Problems?. *Molecular Pharmaceutics*, 2020, 17 (9), pp.3236-3245. 10.1021/acs.molpharmaceut.0c00343 . hal-04560777

**HAL Id: hal-04560777**

**<https://hal.science/hal-04560777>**

Submitted on 26 Apr 2024

**HAL** is a multi-disciplinary open access archive for the deposit and dissemination of scientific research documents, whether they are published or not. The documents may come from teaching and research institutions in France or abroad, or from public or private research centers.

L'archive ouverte pluridisciplinaire **HAL**, est destinée au dépôt et à la diffusion de documents scientifiques de niveau recherche, publiés ou non, émanant des établissements d'enseignement et de recherche français ou étrangers, des laboratoires publics ou privés.

# Cosolvents in Self-Emulsifying Drug Delivery Systems (SEDDS): Do They Really Solve Our Solubility Problems?

Arne Matteo Jörgensen, Julian David Friedl, Richard Wibel, Joseph Chamieh, Hervé Cottet, and Andreas Bernkop-Schnürch\*



Cite This: *Mol. Pharmaceutics* 2020, 17, 3236–3245



Read Online

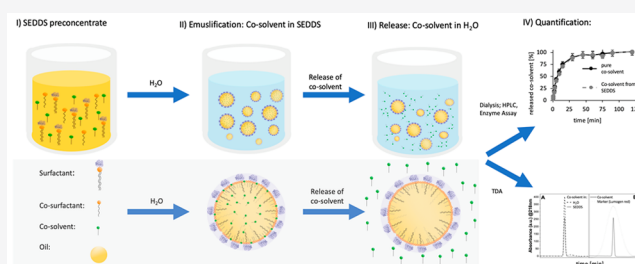
ACCESS |

Metrics & More

Article Recommendations

**ABSTRACT:** The aim of this study was to investigate the fate and the impact of cosolvents in self-emulsifying drug delivery systems (SEDDS). Three different SEDDS comprising the cosolvents DMSO ( $F_D$ ), ethanol ( $F_E$ ), and benzyl alcohol ( $F_{BA}$ ) as well as the corresponding formulations without these cosolvents ( $F_{D0}$ ,  $F_{E0}$ , and  $F_{BA0}$ ) were developed. Mean droplet size, polydispersity index (PDI),  $\zeta$  potential, stability, and emulsification time were determined. Cosolvent release studies were performed via the dialysis membrane method and Taylor dispersion analysis (TDA). Furthermore, the impact of cosolvent utilization on payloads in SEDDS was examined using quinine as a model drug. SEDDS with and without a cosolvent showed no significant differences in droplet size, PDI, and  $\zeta$  potential. The emulsification time was 3-fold ( $F_{D0}$ ), 80-fold ( $F_{E0}$ ), and 7-fold ( $F_{BA0}$ ) longer due to the absence of the cosolvents. Release studies in demineralized water provided evidence for an immediate and complete release of DMSO, ethanol, and benzyl alcohol. TDA confirmed this result. Moreover, a 1.4-fold ( $F_D$ ), 2.91-fold ( $F_E$ ), and 2.17-fold ( $F_{BA}$ ) improved payload of the model drug quinine in the selected SEDDS preconcentrates was observed that dropped after emulsification within 1–5 h due to drug precipitation. In parallel, the quinine concentrations decreased until reaching the same levels of the corresponding SEDDS without cosolvents. Due to the addition of hydrophilic cosolvents, the emulsifying properties of SEDDS are strongly improved. As hydrophilic cosolvents are immediately released from SEDDS during the emulsification process, however, their drug solubilizing properties in the resulting oily droplets are very limited.

**KEYWORDS:** self-emulsifying drug delivery systems (SEDDS), cosolvent release, nanoemulsions, Taylor dispersion analyses (TDA), bioavailability



## 1. INTRODUCTION

One of the most promising tools for oral delivery of poorly water-soluble drugs are lipid-based formulations (LBF). Solid lipid nanoparticles (SLN), nanostructured lipid carriers (NLC), nanoemulsions, and self-emulsifying drug delivery systems (SEDDS) offer improved oral bioavailability for incorporated lipophilic drugs.<sup>1</sup> Among LBFs, in particular, SEDDS are of high industrial relevance. In recent years, these systems have been frequently utilized to enhance oral bioavailability of poorly water-soluble drugs by forming colloidal systems after self-emulsification.<sup>2,3</sup> Indeed, many examples proving oral bioavailability enhancement of drugs incorporated into SEDDS can be found in literature and on the global market.<sup>4,5</sup> The benefit of SEDDS is mainly based on the comparatively high solubility of drugs in the oily droplets during their transit through the gastrointestinal tract.<sup>6–8</sup> Thus, it is required to dissolve drug candidates in the lipid phase of the formulation in order to achieve sufficiently high payloads providing solubility until absorption.<sup>9–11</sup> Lipid-based excipients commonly used in SEDDS include vegetable oils and

their derivatives, which are effortlessly emulsified by surfactants and cosurfactants.<sup>12,13</sup> In order to provide sufficient drug solubility in SEDDS, hydrophilic organic solvents such as glycerol ( $\log P = -1.76$ ), dimethyl sulfoxide (DMSO) ( $\log P = -1.35$ ), ethanol ( $\log P = -0.31$ ), isopropanol ( $\log P = 0.05$ ), or benzyl alcohol (BA) ( $\log P = 1.1$ ) are also utilized.<sup>2,6</sup> With the aid of these cosolvents, it is possible to dissolve most drugs in SEDDS preconcentrates. Nevertheless, it remains questionable whether this approach leads to the desired drug dissolution in the oily droplets of SEDDS after emulsification in aqueous media. Although a fast release of cosolvents from SEDDS and consequently the drop in drug solubility within the oily droplets can be anticipated, the release of such

Received: March 29, 2020

Revised: June 16, 2020

Accepted: July 13, 2020

Published: July 13, 2020



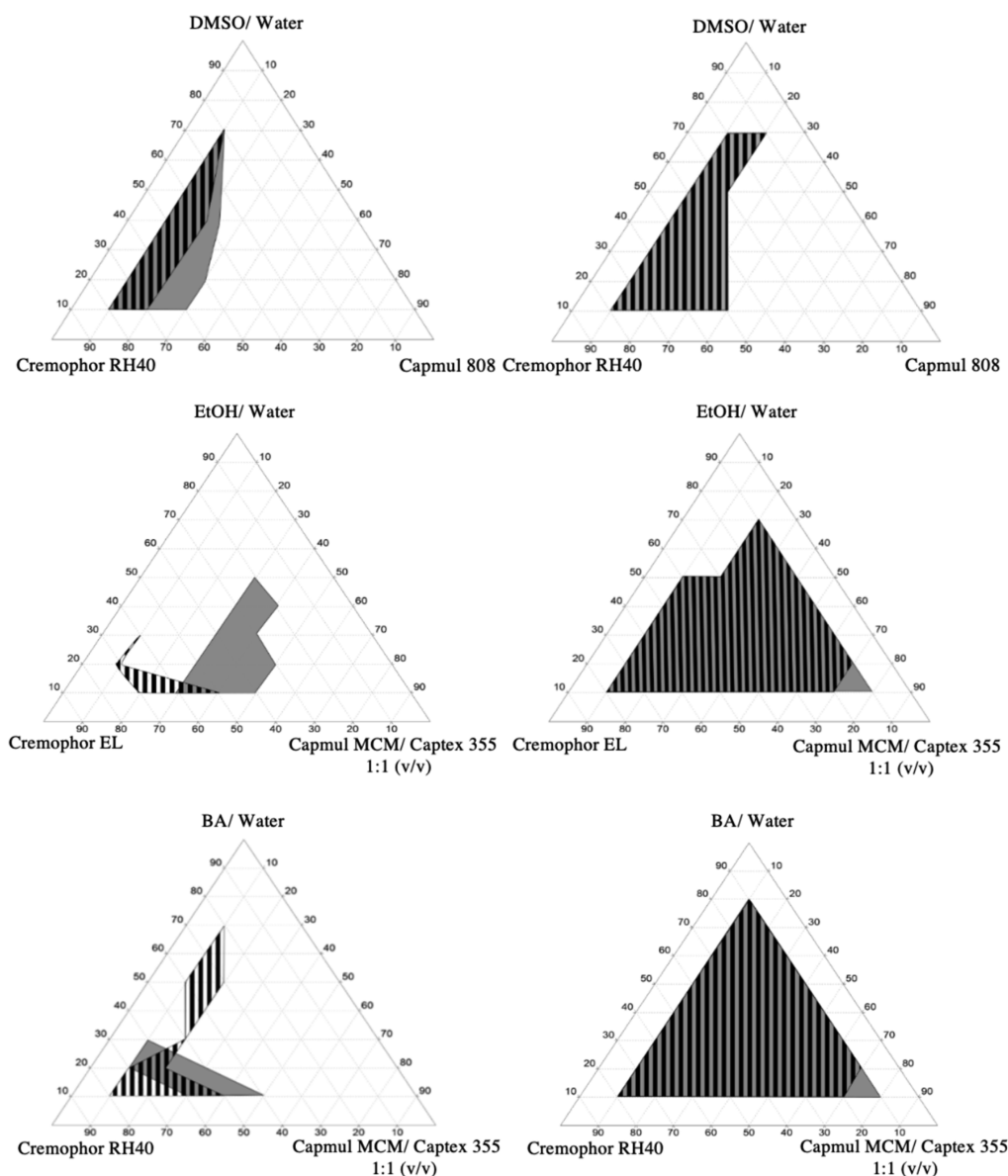


**Figure 1.** Pseudoternary phase diagrams of mixtures with cosolvent (gray area) and without cosolvent (black striped area). Components are represented in percent by volume, and data points depict the region of nanoemulsion. Left-hand side, dilution rates 1:10; right-hand side, dilution rates 1:100 in demineralized water. Indicated values are means ( $n \geq 3$ )  $\pm$  SD.

hydrophilic solvents from SEDDS has so far not been evaluated at all.<sup>7,14</sup>

The aim of this study was, therefore, to investigate the fate of cosolvents in SEDDS after dispersion and to evaluate their impact on SEDDS in general. For this purpose, three different cosolvents listed in decreasing hydrophilicity: DMSO > ethanol > BA were chosen. SEDDS with and without these cosolvents were developed and characterized. Subsequently, cosolvent release studies using a diffusion membrane method as well as Taylor dispersion analysis (TDA) were performed. Furthermore, the model drug quinine ( $\log P = 3.44$ ) was chosen to examine the impact of these cosolvents on drug solubility and release from SEDDS.<sup>15</sup>

## 2. MATERIALS AND METHODS

**2.1. Materials.** Cremophor EL (polyethoxylated-35 castor oil, hydrophilic–lipophilic-balance (HLB) = 13), Cremophor RH40 (polyoxyl 40 hydrogenated castor oil, HLB = 15),

dimethyl sulfoxide (DMSO), ethanol, benzyl alcohol (BA), and quinine anhydrous (99%) were purchased from Sigma-Aldrich (Austria). Capmul MCM EP/NF (glyceryl caprylate/caprate, HLB = 5–6), Capmul 808G EP/NF (glycerol monocaprylate, HLB = 6), and Captex 355 (caprylic/capric triglyceride) were supplied by Abitec (Columbus, USA) as free samples. The Float-A-Lyzer G2 Dialysis Device (MWCO: 20 kDa) was purchased from Fisher Scientific (Schwerte, Germany), and an Ethanol Assay Kit (KA4087) was obtained from Abnova (Taoyuan City, Taiwan).

**2.2. SEDDS Development and Characterization.** In order to develop suitable SEDDS, the nanoemulsion area of mixtures comprising different ratios of surfactant, oil, and cosolvent was determined. Therefore, 100  $\mu$ L of combinations varying from 10 to 80% were prepared using a vortex mixer and a heat gun (60  $^{\circ}$ C). To keep the ratios of oils and surfactants constant, the amounts of cosolvent were substituted by demineralized water. Afterward, 10 or 100  $\mu$ L of the

**Table 1.** Compositions of SEDDS with ( $F_D$ ,  $F_E$ ,  $F_{BA}$ ) and without Cosolvents ( $F_{D0}$ ,  $F_{E0}$ ,  $F_{BA0}$ )<sup>a</sup>

formulation	$F_D$	$F_{D0}$	$F_E$	$F_{E0}$	$F_{BA}$	$F_{BA0}$
Cremporph RH40	37.5	37.5			50	50
Cremporph EL			40	40		
Capmul 808	25	25				
Capmul MCM			15	15	15	15
Captex 355			15	15	15	15
DMSO	37.5	0 <sup>b</sup>				
ethanol			30	0 <sup>b</sup>		
BA					20	0 <sup>b</sup>
mean droplet size [nm]	14.52 ± 0.8	15.6 ± 0.87	25.14 ± 0.38	23.87 ± 0.92	22.35 ± 0.61	22.17 ± 0.47
PDI	0.09 ± 0.03	0.14 ± 0.08	0.03 ± 0.01	0.04 ± 0.01	0.03 ± 0.01	0.05 ± 0.01
ζ potential [mV]	-2.94 ± 0.77	-1.91 ± 0.63	-1.55 ± 0.41	-2.27 ± 0.55	-0.95 ± 0.26	-1.73 ± 0.71
centrifugation test	stable	stable	stable	stable	stable	stable

<sup>a</sup>Values are indicated in percent (v/v). Droplet size, polydispersity index (PDI), and ζ potential were determined in demineralized water at 37 °C (dilution of 1:100). Indicated values are means ( $n \geq 3$ ) ± SD. <sup>b</sup>Cosolvent replaced by the same amount of water.

mixtures were added to 990 or 900 μL of demineralized water, respectively. The droplet size of each blend was assessed after 24 h of storage at room temperature to examine emulsion formation efficiency, utilizing a Zetasizer Nano ZSP (Malvern Instruments, Worcestershire, UK). The area of emulsion formation was evaluated using pseudoternary phase diagrams as described previously with minor modifications to identify suitable SEDDS.<sup>16</sup> Diagrams (Figure 1) were mapped using the software Triplot version 4.1.2. In order to be able to quantify each cosolvent and to emulsify SEDDS in low dilutions with water (1:10) in the dialysis tubes (Float-A-Lyzer, Fischer Scientific, Schwerte, Germany) SEDDS needed to comprise high amounts of the specific cosolvent. Thus, SEDDS were selected from the 1:10 diagrams and prepared as described above. Mean droplet size, polydispersity index, and ζ potential of selected formulations were determined in a dilution of 1:100 by photon correlation spectroscopy utilizing Zetasizer Nano ZSP. Furthermore, centrifugation and dissolution tests were performed.<sup>17</sup> Briefly, SEDDS were centrifuged 30 min at 3500 rpm to examine phase separation. The self-emulsification efficiency was assessed by using a standard USP XXII dissolution apparatus 2 (Erweka, Langen, Germany). Under gentle agitation at 50 rpm of the rotating standard stainless-steel dissolution paddle, 1 mL of pre-concentrate was added to 500 mL of demineralized water at 37 °C. The dissolution time was determined visually.

**2.3. Release Studies.** **2.3.1. Diffusion Membrane Method.** The release of cosolvents from SEDDS was evaluated in demineralized water at 37 °C by using dialysis tubes (Float-A-Lyzer). Therefore, 100 μL of the concentrate of formulation  $F_D$ ,  $F_E$ , and  $F_{BA}$  was emulsified in demineralized water to a total volume of 1 mL. Afterward, the emulsion/solution was dialyzed against 15 mL of demineralized water at 37 °C under shaking at 550 rpm on an Eppendorf ThermoMixer C (Hamburg, Germany). At predetermined time points, 100 μL aliquots were withdrawn from the release medium and replaced by fresh demineralized water.<sup>18</sup> The amount of released cosolvent was quantified via HPLC or the ethanol assay kit as described below. The equivalent volume of the pure cosolvent of the corresponding formulation served as control. Thus, 37.5 μL of DMSO ( $F_D$ ), 30 μL of EtOH ( $F_E$ ), and 20 μL of BA ( $F_{BA}$ ) were dialyzed as described above. Subsequently, the possible hindrance to cosolvent diffusion caused by the dialysis membrane was evaluated by calculating

the amount of a 100% release of each cosolvent. This calculated quantity was set to 100% in the figure.

**2.3.2. Quantification of Cosolvents.** The extent of DMSO and BA release was quantified by HPLC. The system consisted of a Hitachi Chromaster (Tokyo, Japan) equipped with a 5160 pump, 5260 autosampler, 5310 column oven, and 5430 photodiode array UV detector. DMSO was quantified following a slightly modified method described previously.<sup>19</sup> In brief, the stationary phase was a Nucleosil 100–5 C18 column (125 × 4 mm, 5 μm), as the mobile phase served a binary solvent system of water/acetonitrile 85/15 at 40 °C and a 0.6 mL min<sup>-1</sup> flow rate. DMSO was detected at a 195 nm wavelength. BA was quantified according to a method described previously.<sup>20</sup> Therefore, a Nucleosil 100–5 C18 column (250 × 4 mm, 5 μm) was used as a stationary phase. The mobile phase was a binary solvent system of water/acetonitrile 62/38 at a flow rate of 1.2 mL min<sup>-1</sup>. The detector wavelength was set at 254 nm. The enzyme assay kit KA4087 was utilized to quantify the amount of ethanol released. In brief, 50 μL of the ethanol working solution consisting of the Amplitude Ethanol Reagent, the assay buffer, and the ethanol enzyme mix was added to 50 μL of the reagent in a solid black 96-well microplate (Greiner Bio-one, Germany), mixed properly, and incubated 5–30 min at room temperature protected from light. Fluorescence intensity was monitored with a multimode plate reader (Tecan Spark, Tecan Trading AG, Switzerland) at 540 nm excitation and at 590 nm emission wavelengths.

**2.3.3. Taylor Dispersion Analysis.** TDA was performed on an Agilent 7100 CE instrument (Waldbronn, Germany) using fused silica capillaries (Polymicro technologies, USA) having 60 cm × 75 μm i.d. dimensions and a detection window at 51.5 cm for UV. A Zetalif LED induced fluorescence detector (Picometrics, Toulouse, France) was hyphenated in line with a detection window at 48 cm from the injection point. The vial carousel was thermostated using an external circulating water bath, Julabo 600F (Seelbach, Germany). TDA experiments were carried out using 50 mbar mobilization pressure; the samples were injected hydrodynamically by applying a 30 mbar pressure for 4 s. New capillaries were first conditioned with 1 M NaOH for 20 min and water for 10 min and finally flushed with the matrix for 10 min. The operating temperature was set to 37 °C. Before sample analysis, the capillary was previously filled with the matrix (formulations in Table 1) by flushing (application of a pressure of 1 bar) for 150 s. The matrix

volume, used for the prefilling, was between  $\sim 120$  and  $200 \mu\text{L}$  (depending on the formulation and its relative viscosity) corresponding to  $\sim 5$ – $8$  times the total capillary volume. In order to investigate the fate of the cosolvents, the formulations containing cosolvents were injected and mobilized with the formulation without containing the cosolvent of interest. Therefore, the microdroplets of all formulations were fluorescently marked with Lumogen red F300 (BASF) to confirm their presence and to determine their size. The solutes were monitored by UV absorbance at  $218 \text{ nm}$  (DMSO) and  $254 \text{ nm}$  (BA) and by fluorescence with an excitation at  $480 \text{ nm}$ . Emission light was measured through a ball lens and a high-pass filter in the wavelength range from  $515$ – $760 \text{ nm}$ . The Taylorgrams were recorded with the Agilent Chemstation software (Agilent Technologies, Santa Clara, USA).

**2.3.4. Theoretical Aspects of TDA.** TDA is a simple and absolute method, allowing the determination of the molecular diffusion coefficient and of the hydrodynamic radius of a given molecule. It is based on the analysis of the peak broadening of an injected solute plug in an open capillary tube and under a laminar Poiseuille flow.<sup>21</sup> When the injected sample is monodisperse in size, the elution profile, obtained by online UV or fluorescence detection through the capillary tube, is Gaussian according to the following equation:

$$S(t) = \frac{S_0}{\sigma\sqrt{2\pi}} \exp\left[-\frac{(t - t_0)^2}{2\sigma^2}\right] \quad (1)$$

where  $t_0$  is the average elution time [s],  $\sigma^2$  is the temporal variance of the elution profile [ $\text{s}^2$ ], and  $S_0$  is a constant that depends on the response factor and the injected quantity of solute. The band broadening resulting from Taylor dispersion is easily quantified via the temporal variance of the elution profile. The latter is obtained by fitting the experimental data with eq 1. The molecular diffusion coefficient  $D$  of the sample can be calculated using eq 2 and its hydrodynamic radius  $R_h$  calculated using the Stokes–Einstein equation, eq 3:

$$D = \frac{R_c^2 t_0}{24\sigma^2} \quad (2)$$

$$R_h = \frac{k_B T}{6\pi\eta D} \quad (3)$$

where  $R_c$  is the capillary radius [m],  $k_B$  is the Boltzmann constant [ $\text{Pa m}^3 \text{ K}^{-1}$ ],  $T$  is temperature [K], and  $\eta$  is the viscosity of the matrix [ $\text{Pa s}$ ].

Equations 1 and 2 are valid when two conditions are fulfilled. First,  $t_0$  should be much longer than the characteristic diffusion time of the solute in the cross section of the capillary, i.e.,  $t_0 \geq 1.25 R_c^2/D$  for a relative error  $\varepsilon$  on the determination of  $D$  lower than 3%. Second, the axial diffusion should be negligible compared to convection; i.e., the Peclet number  $P_e = R_c u/D$  should be higher than 40 for  $\varepsilon$  lower than 3%, where  $u$  is the linear velocity.<sup>22,23</sup> In the case of the analysis of microemulsions, the capillary is filled with the desired microemulsion, and a small volume of the same microemulsion marked with a hydrophobic marker is injected to measure the diffusion coefficient of the droplets.<sup>24–27</sup>

**2.4. Impact of Cosolvents on Drug Payload.** The impact of cosolvents on drugs was evaluated by analyzing the maximum solubility of the model drug quinine in each excipient used for SEDDS as well as in the final SEDDS preconcentrates with or without cosolvents. Each mixture was

incubated on a thermomixer at room temperature under shaking at  $2000 \text{ rpm}$  for  $24 \text{ h}$ , followed by  $15 \text{ min}$  of centrifugation at  $12\,500 \text{ rpm}$ . Subsequently, quinine was quantified in the saturated supernatants by fluorescence spectroscopy, according to a method described previously.<sup>28</sup> In brief, a calibration curve was generated by measuring standard solutions of anhydrous fluorescence grade quinine ( $\geq 98.0\%$ ) in  $0.05 \text{ M H}_2\text{SO}_4$  ranging from  $1.0$  to  $0.10 \text{ mg/L}$ . In order to determine quinine concentrations in samples,  $10 \mu\text{L}$  of the sample was withdrawn and added to  $990 \mu\text{L}$  of EtOH ( $96\% \text{ v/v}$ ). Afterward, the samples were diluted with  $0.05 \text{ M H}_2\text{SO}_4$ . The fluorescence intensity was measured at  $350 \text{ nm}$  excitation and at  $450 \text{ nm}$  emission wavelengths, utilizing the multimode microplate reader (TECAN). Additionally, the water solubility of quinine at  $37 \text{ }^\circ\text{C}$  was quantified.

**2.5. Drug Release Studies.** Quinine saturated SEDDS with ( $F_D, F_E, F_{BA}$ ) and without cosolvents ( $F_{D0}, F_{E0}, F_{BA0}$ ) were emulsified 1:100 in demineralized water and incubated at  $37 \text{ }^\circ\text{C}$  under shaking at  $550 \text{ rpm}$  on a thermomixer. At predetermined time points, the formed quinine emulsions were centrifuged at  $12\,500 \text{ rpm}$  for  $45 \text{ s}$  before withdrawing  $10 \mu\text{L}$  of aliquots from the supernatant. Afterward, quinine concentrations were determined as described above and plotted against time. In order to examine whether pure cosolvents were able to keep quinine solubilized to the same extent, the initially induced gain in solubility ( $t = 0$ ) was calculated for each SEDDS by using the concentration–time profiles. Subsequently, cosolvent–quinine solutions were prepared accordingly. Quinine concentrations were determined immediately after dissolving the equal volume of cosolvent–quinine solution that was formulated in the corresponding SEDDS ( $3.75 \mu\text{L}$  of DMSO,  $3 \mu\text{L}$  of EtOH, and  $2 \mu\text{L}$  of BA) in EtOH and demineralized water in a total volume of  $1 \text{ mL}$  at  $37 \text{ }^\circ\text{C}$  as described above.

**2.6. Statistical Data Analysis.** Statistical data analyses were performed using the Student's  $t$  test to analyze the significant difference between two mean values assuming unequal variance. The level of  $p \leq 0.05$  was set for significant,  $p \leq 0.01$  for very significant, and  $p \leq 0.001$  for highly significant. The results were expressed as the mean of at least three experiments  $\pm$  standard deviation (SD).

### 3. RESULTS AND DISCUSSION

#### 3.1. SEDDS Development and Characterization.

**3.1.1. Area of Nanoemulsion Formation.** In order to develop suitable SEDDS for cosolvent release studies, nanoemulsion areas of the selected components have been evaluated by pseudoternary phase diagram construction. The resulting diagrams (Figure 1) depict the areas of nanoemulsion formation in dilution rates of 1:10 and 1:100 in demineralized water.

The phase diagrams of 1:10 dilution rate show that blends, in which DMSO and ethanol served as cosolvents, exhibit larger areas of nanoemulsion formation compared to the mixtures without the cosolvent. This effect of cosolvents is well-known and has also been shown in literature before.<sup>29</sup> In theory, the surfactant alone is not able to lower the oil–water interfacial tension to bring the surface tension close to zero, which is necessary to yield an emulsion.<sup>13</sup> The addition of a cosolvent offers the possibility of surfactant reduction to use a minimum concentration in SEDDS. The reduced amount of surfactant leads to increased biocompatibility of the formulation, as it is well-known that large amounts of

surfactants cause GI irritation and acute epithelial damage.<sup>2,29–32</sup>

On the contrary, BA showed a different behavior regarding nanoemulsion formation. Even in high concentrations, BA was not able to lower the surface tension in an efficient manner. The area of nanoemulsion formation was decreased, and consequently, the formulation variability was reduced. Overall, the 1:10 pseudo ternary phase diagrams showed the possibility to emulsify higher amounts of oils by the addition of cosolvents to the mixture, even at lower surfactant concentrations. As the drug candidate should be mainly dissolved in the oily phase of SEDDS, higher payloads are expected. Furthermore, the enlarged nanoemulsion areas imply an increased variability for excipient ratios facilitating the development of SEDDS that emulsify even in low dilution with aqueous media. Hence, it would be beneficial to add cosolvents when formulating SEDDS intended for applications in body regions with limited access to body fluids such as the vaginal, nasal, or ocular mucosa. In higher dilution rates (1:100), the cosolvent effect of nanoemulsion formation area enlargement was negligible. Mixtures with and without cosolvents were able to form nanoemulsions regardless of the concentrations of oil and surfactant. Blends comprising DMSO showed the smallest enlargement compared to mixtures containing ethanol and BA. An explanation for this difference in nanoemulsion formation can be given by the used oils. Capmul 808 EP/NF served as the oily phase in DMSO blends, consisting solely of glycerol monocaprylate (HLB = 6). On the contrary, ethanol and BA blends contained Capmul MCM EP/NF, a mixture of mono- and diglycerides (glyceryl caprylate/caprate). It is known, that mixtures of medium-chain mono- and diglycerides exhibit a much higher solubilization and emulsification potential compared to medium-chain triglycerides.<sup>13</sup> Recently, studies of Nornoo et al. have also shown the possibility to formulate medium-chain mono- and diglycerides based microemulsions even without any additional surfactant.<sup>33,34</sup>

**3.1.2. Selection of SEDDS.** Based on the pseudoternary phase diagrams, SEDDS were selected and characterized. The determined characteristics are summarized in Table 1.

SEDDS containing a cosolvent ( $F_D$ ,  $F_E$ , and  $F_{BA}$ ) compared to formulations omitting the cosolvent ( $F_{D0}$ ,  $F_{E0}$ , and  $F_{BA0}$ ) showed no significant differences in droplet size and PDI, although accounting 20–37.5% of the formulation. Hence, it seems likely that they are not an integral part of the system. There was neither influence on the stability nor the  $\zeta$  potential observed. With and without cosolvents, the determined  $\zeta$  potentials were close to zero, since all tested SEDDS comprised noncharged excipients solely. Consequently, improved stability of the formed nanoemulsions due to electric repulsion cannot be expected.

**3.1.3. Self-Emulsification Time.** Formulations containing cosolvents ( $F_D$ ,  $F_E$ , and  $F_{BA}$ ) rapidly formed nanoemulsions. On the contrary, formulations without cosolvents ( $F_{D0}$ ,  $F_{E0}$ , and  $F_{BA0}$ ) needed more time to emulsify entirely as shown in Figure 2 below.

$F_{D0}$  exhibited a 3-fold longer emulsification time compared to the corresponding formulation with DMSO ( $F_D$ ),  $F_{E0}$  compared to  $F_E$  80-fold, and  $F_{BA0}$  compared to  $F_{BA}$  7-fold. Thus, the blending of cosolvents and water-soluble surfactants facilitated the formulations of emulsification in the aqueous phase. The cosolvents successively impart the flexibility of the hydrophobic tails of the surfactant leading to a faster

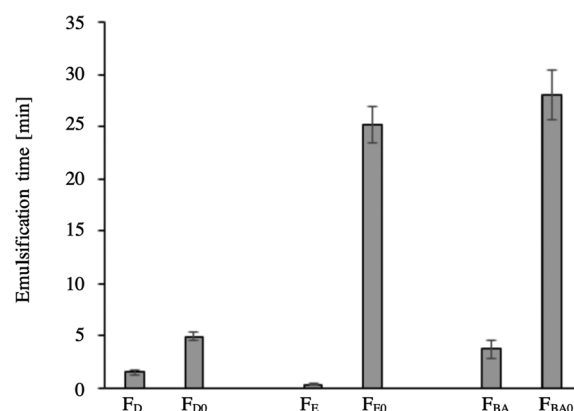


**Figure 2.** Emulsification time in minutes of 1 mL preconcentrate of formulations with cosolvents ( $F_D$ ,  $F_E$ ,  $F_{BA}$ ) and without ( $F_{D0}$ ,  $F_{E0}$ ,  $F_{BA0}$ ) in 500 mL of demineralized water at 37 °C under gentle agitation at 50 rpm of the rotation standard stainless-steel dissolution paddle. Indicated values are means ( $n \geq 3$ )  $\pm$  SD.

dissolution and emulsification time of SEDDS.<sup>2,13,30,35,36</sup> Especially amphiphilic, short-chain cosolvents are able to interact with the surfactant monolayers at the interface modifying their packing.<sup>13,30,37</sup> Without cosolvents, the surfactant–oil surface forms a viscous liquid crystalline or gel crystalline phase, requiring more time to emulsify completely.<sup>2</sup> Studies of Pouton et al. also proved that high surfactant concentrations decelerate self-emulsification time requiring more energy to disperse.<sup>38</sup> Consequently, a sustained drug release affecting bioavailability and likely causing an enhanced risk of side effects such as GIT irritations or damage of the gastric or intestinal mucosa can be anticipated.<sup>2</sup>

**3.2. Release Studies.** **3.2.1. Diffusion Membrane.** The release of the cosolvents is illustrated in Figure 3. One hundred percent was set to the calculated maximum amount of possible cosolvent release into the release medium.

The release profile of pure, unformulated DMSO and ethanol (Figure 3A,B) shows an immediate and complete release through the dialysis membrane into the release medium within 60 min. In comparison to the release of the corresponding SEDDS ( $F_D$  and  $F_E$ ), no difference to the pure cosolvent was obtained. On the contrary,  $F_{BA}$  (Figure 3C) shows a sustained release of the cosolvent compared to the unformulated, pure BA. Even though the release into the aqueous phase beyond the membrane was completed after 3 h in both cases, there was a slight difference in their deliverance. After 25 min, 50% of pure BA was set free, whereas only 25% BA from  $F_{BA}$  was found in the release medium. This sustained release is likely provided by physical and chemical interactions between the cellulose ester membrane of the dialysis tube, surfactant, and cosolvent. Surfactants adsorb and accumulate in interfacial regions of membranes and alter the permeability of the membrane.<sup>39,40</sup> Consequently, adsorption and desorption processes as well as hydrogen bond formation between cosolvent and membrane constitute a bigger hindrance for the release of BA. Paired with low hydrophilicity ( $\log P = 1.1$ ) and moderate solubility in water ( $4 \text{ g } 100 \text{ mL}^{-1}$  at 25 °C), the diffusion celerity of BA from the SEDDS droplet to the aqueous release medium is additionally limited.<sup>41</sup> Thus, a slight deceleration of BA release was obtained.

**3.2.2. Taylor Dispersion.** In order to confirm the previous results, TDA was applied to qualitatively localize the cosolvents

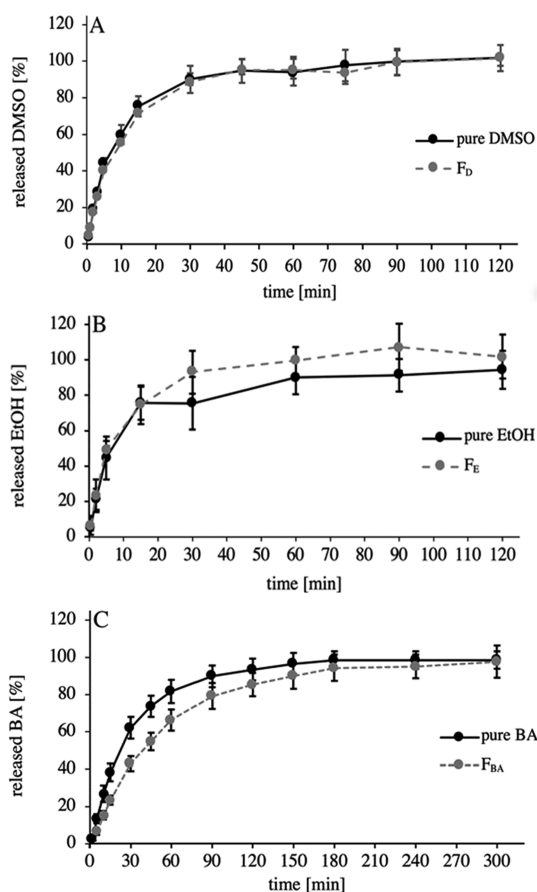


**Figure 3.** Cosolvent release from formulations F<sub>D</sub> (A), F<sub>E</sub> (B), and F<sub>BA</sub> (C) compared to pure cosolvents. 100  $\mu$ L of SEDDS preconcentrate and the equivalent volume of the pure cosolvent as a control, respectively, were dissolved in demineralized water to a total volume of 1 mL and dialyzed against 15 mL of demineralized water at 37 °C under shaking at 550 rpm. Indicated values are means ( $n \geq 3$ )  $\pm$  SD.

immediately after the emulsification of the SEDDS preconcentrate in demineralized water (Figure 4).

In case the cosolvent is not incorporated in the droplets of the SEDDS, an elution profile corresponding to the dispersion of the cosolvent in the continuous phase, i.e., water, would be obtained (Figure 4, A black dashed trace) according to the size of the pure cosolvent in the continuous phase. On the contrary, if the cosolvent remains inside the droplet, a dispersion profile corresponding to a larger object than the cosolvent itself would be observed. As a matter of comparison, the size of the droplets was determined in the presence and the absence of the cosolvent. For this purpose, Lumogen red F300 was used as a hydrophobic marker ( $\log P = 17.60$ ) and was prepared in all the formulations, which allowed to determine the droplet size of the formulations (Figure 4, B black dotted trace). Additionally, the hydrodynamic diameter of pure DMSO and BA were determined independently by TDA in water. The results are gathered in Table 2.

As can be seen from Table 2, the results of the TDA agree very well with the ones obtained utilizing the Zetasizer Nano ZSP (Table 1). The localization of cosolvents was observed by injecting the formulations containing the cosolvent and the fluorescent marker and mobilizing them with the ones without the cosolvent (Figure 4, gray traces). The obtained elution profile corresponded to the profile of the cosolvent in

demineralized water and showed that the cosolvents are quantitatively outside of the SEDDS. The apparent hydrodynamic diameters for the formulations F<sub>D</sub> and F<sub>BA</sub> using the cosolvent as a marker were 0.20 and 0.63 nm, respectively, corresponding to the sizes of the cosolvents in demineralized water. It is important to note that the peaks were obtained at the earliest 10 min after emulsification at 37 °C, and no significant peak evolution was observed after several hours. Formulation F<sub>E</sub> does not possess the experimental requirements to be analyzed via TDA in the same manner due to the lack of UV visibility of the utilized cosolvent ethanol. However, since EtOH has an intermediate polarity between DMSO and BA, it can be expected to show the same behavior of being immediately released into the aqueous phase after emulsification.

Taken all, both methods showed the evidence of an immediate and complete cosolvent release from SEDDS. It implies that, after the emulsification of the preconcentrate, the cosolvent is no longer part of the formed nanoemulsion droplets. Consequently, loss of solvent capacity occurs. It is already known that cosolvent utilization increases the risk of precipitation upon dilution with aqueous fluids.<sup>6</sup> This effect was shown by the work of Moshin et al. and Dai et al.,<sup>7,14</sup> In order to investigate the consequence of the entire cosolvent release from SEDDS, their impact on drug solubility and release was studied on the model drug quinine.

Moreover, it has to be mentioned that there is still a huge lack of appropriate methods to obtain in vitro drug release from SEDDS.<sup>42</sup> This was even the case in the release study of the small solvent molecule BA that obviously showed a common limitation of membrane diffusion methods due to membrane fouling caused by surfactants.

**3.3. Impact of Cosolvents on Drug Payload.** At first, the maximum solubility of the model drug quinine was determined in each SEDDS component (Figure 5).

The highest quinine solubility was observed in the hydrophilic cosolvents. The alkaloid was very soluble in BA ( $1021.59 \pm 75.34$  mg/mL) and freely soluble in EtOH ( $753.33 \pm 55.37$  mg/mL) and in DMSO ( $288.15 \pm 38.23$  mg/mL). In the oils Capmul 808 ( $191.52 \pm 21.53$  mg/mL) and Capmul MCM ( $177.48 \pm 20.88$  mg/mL), quinine also showed free solubility. On the contrary, the lowest solubility of quinine was determined in the surfactants Cremophor RH40 ( $9.35 \pm 0.95$  mg/mL) and Cremophor EL ( $14.81 \pm 0.55$  mg/mL) followed by the oil Captex 355 ( $7.27 \pm 0.76$  mg/mL). As pure Cremophor RH40 is solid at room temperature, it was not feasible to determine the solubility in this excipient. The determined solubility of quinine in demineralized water was in accordance with the value found in literature.<sup>43</sup>

Second, the solubility of quinine was determined in each SEDDS preconcentrate as listed in Table 1. The results of this study are shown in Figure 6.

Compared to the corresponding SEDDS without cosolvents, F<sub>D</sub> showed the lowest improvement by 1.4-fold, followed by F<sub>E</sub> and F<sub>BA</sub> in which the payload could be improved 2.91-fold and 2.17-fold, respectively. As the highest quinine solubility was observed in BA (Figure 5), the highest quinine solubility was expected in F<sub>BA</sub>. However, the experimentally determined concentration showed that this is not the case (Figure 6). This observation might be explained by the unpredictable complex solubilizing potential of solvent mixtures as blending can lead to increased or decreased drug solubility.<sup>44</sup>

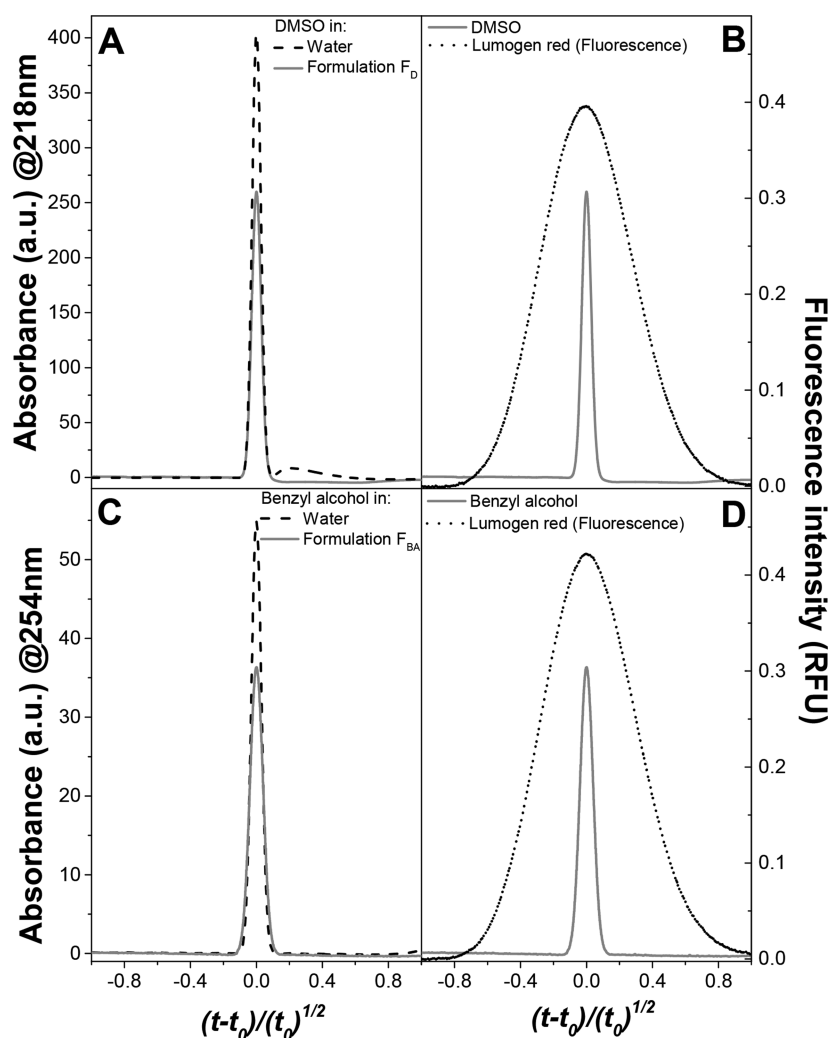


**Figure 4.** Taylor dispersion analysis of formulation  $F_D$  (A, B) and  $F_{BA}$  (C, D) to assess the fate of the cosolvent. Samples: DMSO in water (A, black dashed trace) and in formulation  $F_D$  (A and B, gray traces); BA in water (C, black dashed trace) and in formulation  $F_{BA}$  (C and D, gray traces); Lumogen red in formulation  $F_D$  (B, black dotted trace) and in formulation  $F_{BA}$  (D, black dotted trace). The  $x$ -axis was normalized for better visual comparison.

**Table 2.** Hydrodynamic Diameter ( $D_h$ ) of SEDDS and Pure Cosolvents Determined via TDA<sup>a</sup>

formulation	$F_D$	$F_{D0}$	$F_E$	$F_{E0}$	$F_{BA}$	$F_{BA0}$
$D_h$ SEDDS [nm]	18.17 ± 0.43	17.08 ± 0.12	19.35 ± 0.10	19.54 ± 0.09	22.79 ± 0.17	18.19 ± 0.16
$D_h$ cosolvent [nm]	0.207 ± 0.002				0.63 ± 0.01	

<sup>a</sup>Indicated values are means ( $n \geq 3$ ) ± SD.

Moreover, it was evaluated whether the increased payload in SEDDS pre-concentrates also provides higher drug concentrations in the oily droplets after emulsification. Thus, the tendency of quinine to precipitate from SEDDS was assessed under nonsink conditions as recommended for supersaturated drug delivery systems, allowing adequate investigations of drug precipitation and providing a meaningful in vitro–in vivo correlation.<sup>45–49</sup>

The concentration–time profiles of quinine release from each formulation are illustrated in Figure 7.

Profiles of SEDDS without the cosolvent ( $F_{D0}$ ,  $F_{E0}$ , and  $F_{BA0}$ ) indicated stable quinine concentrations above the maximum quinine solubility in demineralized water. As no precipitation occurred, the retention of the model drug in the oily droplets is likely. In contrast, SEDDS comprising

cosolvents ( $F_D$ ,  $F_E$ , and  $F_{BA}$ ) showed a decrease in quinine concentration over time. In the case of  $F_D$  and  $F_E$ , quinine partially precipitated within 1–1.5 h until the concentration of the corresponding SEDDS without the cosolvent was reached, whereas, in  $F_{BA}$ , quinine remained solubilized in a higher concentration up to 4–5 h.

Results shown in Figure 8 prove that cosolvents alone are not able to keep quinine solubilized to the same extent. Each quinine–cosolvent solution showed a decreased quinine concentration after dissolution in demineralized water (light gray columns) compared to the concentration determined after dissolution in EtOH (gray columns). Immediately after the addition of the cosolvent–quinine solution to demineralized water, quinine precipitated, and thus, the concentration dropped to the maximum solubility in water.



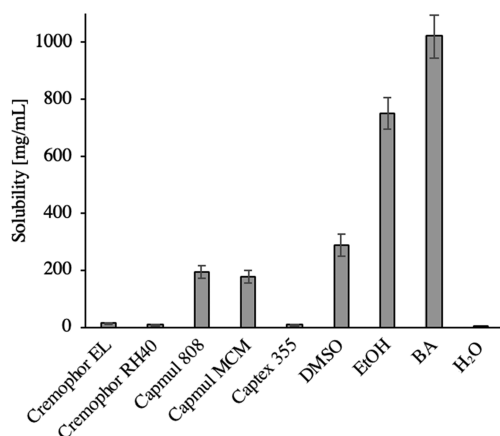


**Figure 5.** Maximum solubility of quinine in each SEDDS component and in demineralized water after 24 h of incubation at room temperature while shaking on a thermomixer at 550 rpm. Indicated values are means ( $n \geq 3$ )  $\pm$  SD.

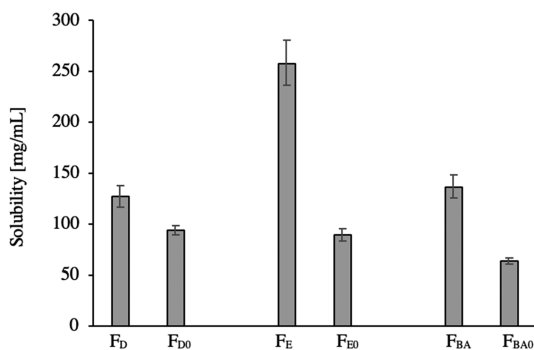


**Figure 6.** Maximum solubility of quinine in SEDDS preconcentrates after 24 h of incubation at room temperature while shaking at 550 rpm. Indicated values are means ( $n \geq 3$ )  $\pm$  SD.

It can be assumed that the combination of cosolvents and SEDDS generates a thermodynamically unstable state of supersaturation, leading to a time-dependent precipitation process of quinine. Such metastable states can improve bioavailability only when remaining stable until absorption. In order to prolong this supersaturation, state precipitation inhibitors can be added to SEDDS, turning them into supersaturated drug delivery systems.<sup>46</sup> Although this approach may prevent drug precipitation, the loss of carrier system related benefits such as protection from hydrolysis and from enzymatic degradation as well as an enhanced mucus permeation has to be taken into consideration. Likewise, an amorphous precipitation state could positively affect drug bioavailability as long as the drug is not prone to instability in body fluids. The concentration–time profiles (Figure 7) indicate the following: the less hydrophilic the cosolvent is, the more time the drug needs to precipitate. Thus, the use of less water-miscible cosolvents of higher lipophilicity such as benzyl benzoate or ethyl acetate could be a promising strategy to avoid precipitation, as these cosolvents can, on the one hand, provide sufficient drug solubility and, on the other hand, remain in the oily droplets for a prolonged period of time. The model drug quinine showed sufficient solubility also in other components of SEDDS. In the case of other drug candidates that are solely soluble in hydrophilic cosolvents, however, a sufficient drug solubility cannot be provided without them. It seems likely that even SEDDS products on the global market

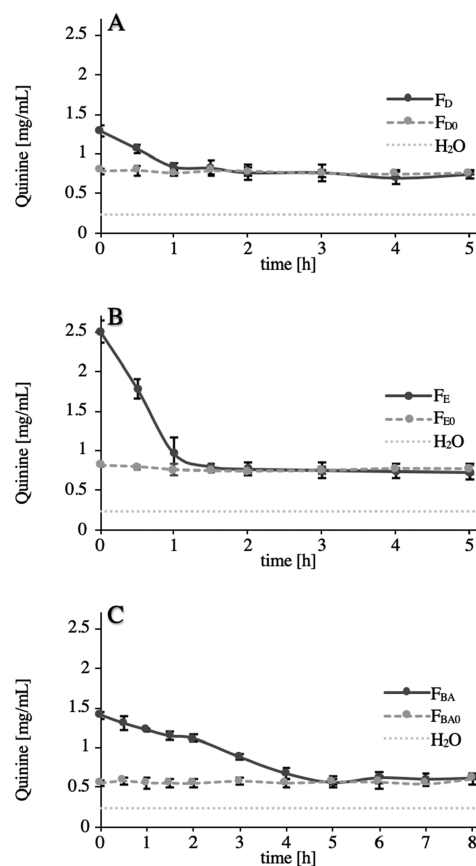


**Figure 7.** Concentration–time profiles of quinine release determined for F<sub>D</sub>/F<sub>D0</sub> (A), F<sub>E</sub>/F<sub>E0</sub> (B), and F<sub>BA</sub>/F<sub>BA0</sub> (C) after emulsification in demineralized water at 37 °C (1:100) while shaking on a thermomixer at 550 rpm. Indicated values are means ( $n \geq 3$ )  $\pm$  SD.

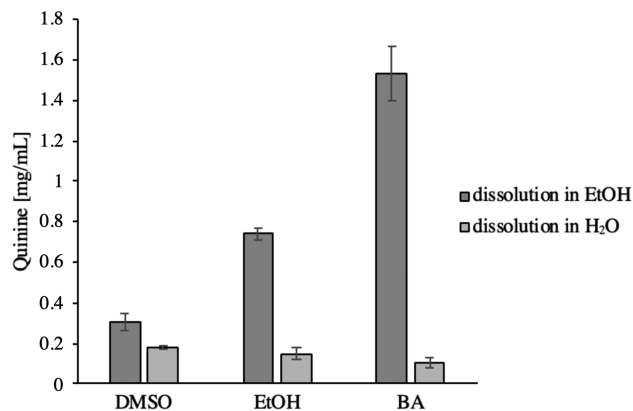


**Figure 8.** Cosolvent–quinine solutions were dissolved in EtOH (dark gray column) and demineralized water (light gray column) in the same amount that was formulated in 10  $\mu$ L of SEDDS (3.75  $\mu$ L of DMSO (F<sub>D</sub>), 3  $\mu$ L of EtOH (F<sub>E</sub>), and 2  $\mu$ L of BA (F<sub>BA</sub>), respectively). The total volume was 1 mL at 37 °C. Indicated values are means ( $n \geq 3$ )  $\pm$  SD.

like Sandimmune Neoral containing the hydrophilic cosolvents ethanol and propylene glycol do not reach their full potential due to this cosolvent problematic.

Adequate payloads in conventional SEDDS can likely only be generated by using drugs being sufficiently soluble in components that remain in the delivery system upon emulsification.

## 4. CONCLUSION

Within this study, the impact of cosolvents in SEDDS was examined. The use of suitable cosolvents can facilitate the development of SEDDS that emulsify already upon low dilution with aqueous media within a comparatively short period of time. Furthermore, the assumption to achieve sufficient payloads with the aid of cosolvents was investigated. The results of our study showed that this assumption is questionable as the tested cosolvents were immediately released from SEDDS after emulsification into the aqueous medium. Consequently, their function to guarantee high payloads in the oily droplets of SEDDS is no longer provided. This hypothesis was confirmed by using quinine as a model drug. Hydrophilic organic solvents rather pretend a solubility enhancement by solely increasing the drug solubility in SEDDS preconcentrate, leading to drug precipitation upon dispersion. However, as the examined cosolvents covered solely log P values from  $-1.35$  to  $1.1$ , less hydrophilic cosolvents like benzyl benzoate might be more promising alternatives.

## AUTHOR INFORMATION

### Corresponding Author

**Andreas Bernkop-Schnürch** – Department of Pharmaceutical Technology, Center for Chemistry and Biomedicine, University of Innsbruck, Institute of Pharmacy, 6020 Innsbruck, Austria; [orcid.org/0000-0003-4187-8277](https://orcid.org/0000-0003-4187-8277); Phone: +43-512-507-58-600; Email: [Andreas.Bernkop@uibk.ac.at](mailto:Andreas.Bernkop@uibk.ac.at); Fax: +43-512-507-58699

### Authors

**Arne Matteo Jörgensen** – Department of Pharmaceutical Technology, Center for Chemistry and Biomedicine, University of Innsbruck, Institute of Pharmacy, 6020 Innsbruck, Austria

**Julian David Friedl** – Department of Pharmaceutical Technology, Center for Chemistry and Biomedicine, University of Innsbruck, Institute of Pharmacy, 6020 Innsbruck, Austria

**Richard Wibel** – Department of Pharmaceutical Technology, Center for Chemistry and Biomedicine, University of Innsbruck, Institute of Pharmacy, 6020 Innsbruck, Austria

**Joseph Chamieh** – IBMM, University of Montpellier, 34095 Montpellier, France; [orcid.org/0000-0003-4209-1337](https://orcid.org/0000-0003-4209-1337)

**Hervé Cottet** – IBMM, University of Montpellier, 34095 Montpellier, France; [orcid.org/0000-0002-6876-175X](https://orcid.org/0000-0002-6876-175X)

Complete contact information is available at:

<https://pubs.acs.org/10.1021/acs.molpharmaceut.0c00343>

### Notes

The authors declare no competing financial interest.

## ACKNOWLEDGMENTS

The authors wish to thank Prof. Albin Kristl, Faculty of Pharmacy, University of Ljubljana, for an inspiring discussion on this topic. The Centre for International Cooperation & Mobility (ICM) of the Austrian Agency for International Cooperation in Education and Research (OeAD-GmbH) has selected this project for support (project no. FR 13/2020). The financial support was provided by the Federal Ministry of Education, Science, and Research (BMBWF). The authors would like to acknowledge this support as well as the support of the French Ministry of Foreign Affairs (MAEE) and the French Ministry for Higher Education and Research (MESR) (Project PHC AMADEUS 2020 N°44090VA).

## REFERENCES

- (1) Pouton, C. W. Formulation of poorly water-soluble drugs for oral administration: Physicochemical and physiological issues and the lipid formulation classification system. *Eur. J. Pharm. Sci.* **2006**, *29*, 278–287.
- (2) Pouton, C. W.; Porter, C. J.H. Formulation of lipid-based delivery systems for oral administration: Materials, methods and strategies. *Adv. Drug Delivery Rev.* **2008**, *60*, 625–637.
- (3) Hauss, D. J. Oral lipid-based formulations. *Adv. Drug Delivery Rev.* **2007**, *59*, 667–676.
- (4) Mahmood, A.; Bernkop-Schnürch, A. SEDDS: A game changing approach for the oral administration of hydrophilic macromolecular drugs. *Adv. Drug Delivery Rev.* **2019**, *142*, 91.
- (5) Neslihan Gursoy, R.; Benita, S. Self-emulsifying drug delivery systems (SEDDS) for improved oral delivery of lipophilic drugs. *Biomed. Pharmacother.* **2004**, *58*, 173–182.
- (6) Shah, S. M.; Jain, A. S.; Kaushik, R.; Nagarsenker, M. S.; Nerurkar, M. J. Preclinical formulations: insight, strategies, and practical considerations. *AAPS PharmSciTech* **2014**, *15*, 1307–23.
- (7) Mohsin, K.; Long, M. A.; Pouton, C. W. Design of Lipid-Based Formulations for Oral Administration of Poorly Water-Soluble Drugs: Precipitation of Drug after Dispersion of Formulations in Aqueous Solution. *J. Pharm. Sci.* **2009**, *98*, 3582–3595.
- (8) Pouton, C. W. Lipid formulations for oral administration of drugs: non-emulsifying, self-emulsifying and ‘self-microemulsifying’ drug delivery systems. *Eur. J. Pharm. Sci.* **2000**, *11*, S93.
- (9) Malcolmson, C.; Lawrence, M. J. A comparison of the incorporation of model steroids into non-ionic micellar and microemulsion systems. *J. Pharm. Pharmacol.* **1993**, *45*, 141–143.
- (10) Malcolmson, C.; Satra, C.; Kantaria, S.; Sidhu, A.; Jayne Lawrence, M. Effect of oil on the level of solubilization of testosterone propionate into nonionic oil-in-water microemulsions. *J. Pharm. Sci.* **1998**, *87*, 109–116.
- (11) Warisnoicharoen, W.; Lansley, A. B.; Lawrence, M. J. Nonionic oil-in-water microemulsions: The effect of oil type on phase behaviour. *Int. J. Pharm.* **2000**, *198*, 7–27.
- (12) Strickley, R. G. *Pharm. Res.* **2004**, *21*, 201.
- (13) Date, A. A.; Nagarsenker, M. S. Parenteral microemulsions: An overview. *Int. J. Pharm.* **2008**, *355*, 19–30.
- (14) Dai, W.-G.; Dong, L. C.; Shi, X.; Nguyen, J.; Evans, J.; Xu, Y.; Creasey, A. A. Evaluation of drug precipitation of solubility-enhancing liquid formulations using milligram quantities of a new molecular entity (NME). *J. Pharm. Sci.* **2007**, *96*, 2957–2969.
- (15) Martin, Y. C. Exploring QSAR: Hydrophobic, electronic, and steric constants. *J. Med. Chem.* **1996**, *39*, 1189.
- (16) Choi, Y. W.; Yeom, D. W.; Song, Y. S.; Kim, S. R.; LEE, S. G.; Kang, M. H.; LEE, S. K. Development and optimization of a self-microemulsifying drug delivery system for atorvastatin calcium by using D-optimal mixture design. *Int. J. Nanomed.* **2015**, *3865*.
- (17) Shafiq, S.; Shakeel, F.; Talegaonkar, S.; Ahmad, F. J.; Khar, R. K.; Ali, M. Development and bioavailability assessment of ramipril nanoemulsion formulation. *Eur. J. Pharm. Biopharm.* **2007**, *66*, 227–243.
- (18) Zupančič, O.; Partenhauser, A.; Lam, H. T.; Rohrer, J.; Bernkop-Schnürch, A. Development and in vitro characterisation of an oral self-emulsifying delivery system for daptomycin. *Eur. J. Pharm. Sci.* **2016**, *81*, 129.
- (19) Thumm, W.; Freitag, D.; Kettrup, A. Determination and quantification of dimethyl sulfoxide by HPLC. *Chromatographia* **1991**, *32*, 461–462.
- (20) Di Pietra, A. M.; Cavrini, V.; Raggi, M. A. Determination of benzaldehyde traces in benzyl alcohol by liquid chromatography (HPLC) and derivative UV spectrophotometry. *Int. J. Pharm.* **1987**, *35*, 13–20.
- (21) Taylor, G. I. Dispersion of soluble matter in solvent flowing slowly through a tube. *Proc. R. Soc. London. Ser. A. Math. Phys. Sci.* **1953**, *219*, 186–203.

- (22) Cottet, H.; Biron, J.-P.; Martin, M. On the optimization of operating conditions for Taylor dispersion analysis of mixtures. *Analyst* **2014**, *139*, 3552–3562.
- (23) Taylor, G. I. Conditions under which dispersion of a solute in a stream of solvent can be used to measure molecular diffusion. *Proc. R. Soc. London. Ser. A. Math. Phys. Sci.* **1954**, *225*, 473–477.
- (24) Chamieh, J.; Davanier, F.; Jannin, V.; Demarne, F.; Cottet, H. Size characterization of commercial micelles and microemulsions by Taylor dispersion analysis. *Int. J. Pharm.* **2015**, *492*, 46–54.
- (25) Chamieh, J.; Jannin, V.; Demarne, F.; Cottet, H. Hydrodynamic size characterization of a self-emulsifying lipid pharmaceutical excipient by Taylor dispersion analysis with fluorescent detection. *Int. J. Pharm.* **2016**, *513*, 262–269.
- (26) Chamieh, J.; Merdassi, H.; Rossi, J.-C.; Jannin, V.; Demarne, F.; Cottet, H. Size characterization of lipid-based self-emulsifying pharmaceutical excipients during lipolysis using Taylor dispersion analysis with fluorescence detection. *Int. J. Pharm.* **2018**, *537*, 94–101.
- (27) Chamieh, J.; Domenech Tarrat, A.; Doudou, C.; Jannin, V.; Demarne, F.; Cottet, H. Peptide release from SEDDS containing hydrophobic ion pair therapeutic peptides measured by Taylor dispersion analysis. *Int. J. Pharm.* **2019**, *559*, 228–234.
- (28) Lawson-Wood, K.; Evans, K. Quinine Fluorescence Determination of Quinine in Tonic Water; *PerkinElmer Appl. Note - Fluoresc. Spectrosc.*, 2013; p 1
- (29) Trotta, M.; Pattarino, F.; Grosa, G. Formation of lecithin-based microemulsions containing n-alkanol phosphocholines. *Int. J. Pharm.* **1998**, *174*, 253–259.
- (30) Lawrence, M. J.; Rees, G. D. Microemulsion-based media as novel drug delivery systems. *Adv. Drug Delivery Rev.* **2000**, *45*, 89–121.
- (31) Li, P.; Ghosh, A.; Wagner, R. F.; Krill, S.; Joshi, Y. M.; Serajuddin, A. T.M. Effect of combined use of nonionic surfactant on formation of oil-in-water microemulsions. *Int. J. Pharm.* **2005**, *288*, 27–34.
- (32) Swenson, E. S.; Milisen, W. B.; Curatolo, W. Intestinal Permeability Enhancement: Efficacy, Acute Local Toxicity, and Reversibility. *Pharm. Res.* **1994**, *11*, 1132–1142.
- (33) Nornoo, A. O.; Chow, D. S.-L. Cremophor-free intravenous microemulsions for paclitaxel: II. Stability, in vitro release and pharmacokinetics. *Int. J. Pharm.* **2008**, *349*, 117–123.
- (34) Nornoo, A. O.; Osborne, D. W.; Chow, D. S.-L. Cremophor-free intravenous microemulsions for paclitaxel: I: Formulation, cytotoxicity and hemolysis. *Int. J. Pharm.* **2008**, *349*, 108–116.
- (35) Rao Baratam, S.; Swamy Padavala, V.; Vijaya Ratna, J. a Promising Approach To Enhance Solubility and Bioavailability By Self Emulsifying Drug Delivery System: a Brief Review. *Innoriginal International Journal of Sciences* **2018**, *5*, 1.
- (36) Trotta, M.; Gallarate, M.; Pattarino, F.; Carlotti, M. E. Investigation of the phase behaviour of systems containing lecithin and 2-acyl lysolecithin derivatives. *Int. J. Pharm.* **1999**, *190*, 83–89.
- (37) Vandamme, T. F. Microemulsions as ocular drug delivery systems: Recent developments and future challenges. *Prog. Retinal Eye Res.* **2002**, *21*, 15–34.
- (38) Pouton, C. W. Formulation of self-emulsifying drug delivery systems. *Adv. Drug Delivery Rev.* **1997**, *25*, 47.
- (39) Tiwari, A. K.; Khan, Z. F. Ion Transport through Surfactant Modified Cellulose Acetate Phthalate Membrane in Acidic Medium. *Int. J. Appl. Sci. Biotechnol.* **2017**, *5*, 267–272.
- (40) Dickhout, J. M.; Virga, E.; Lammertink, R. G. H.; de Vos, W. M. Surfactant specific ionic strength effects on membrane fouling during produced water treatment. *J. Colloid Interface Sci.* **2019**, *556*, 12.
- (41) Scognamiglio, J.; Jones, L.; Vitale, D.; Letizia, C. S.; Api, A. M. Fragrance material review on benzyl alcohol. *Food Chem. Toxicol.* **2012**, *50*, S140–S160.
- (42) Bernkop-Schnürch, A.; Jalil, A. Do drug release studies from SEDDS make any sense? *J. Controlled Release* **2018**, *271*, 55.
- (43) Samuel, H.; Yalkowsky, R. M. D. Aquasol database of aqueous solubility. *Coll. Pharmacy, Univ. Arizona, Tucson, AZ.* **1992**, 189, 499.
- (44) Ruether, F.; Sadowski, G. Modeling the solubility of pharmaceuticals in pure solvents and solvent mixtures for drug process design. *J. Pharm. Sci.* **2009**, *98*, 4205–4215.
- (45) Bevernage, J.; Brouwers, J.; Brewster, M. E.; Augustijns, P. Evaluation of gastrointestinal drug supersaturation and precipitation: Strategies and issues. *Int. J. Pharm.* **2013**, *453*, 25–35.
- (46) Augustijns, P.; Brewster, M. E. Supersaturating drug delivery systems: Fast is not necessarily good enough. *J. Pharm. Sci.* **2012**, *101*, 7–9.
- (47) Van Speybroeck, M.; Mellaerts, R.; Mols, R.; Thi, T. D.; Martens, J. A.; Van Humbeeck, J.; Annaert, P.; Van den Mooter, G.; Augustijns, P. Enhanced absorption of the poorly soluble drug fenofibrate by tuning its release rate from ordered mesoporous silica. *Eur. J. Pharm. Sci.* **2010**, *41*, 623–630.
- (48) Dong, W. Y.; Maincent, P.; Bodmeier, R. In vitro and in vivo evaluation of carbamazepine-loaded enteric microparticles. *Int. J. Pharm.* **2007**, *331*, 84.
- (49) Brouwers, J.; Brewster, M. E.; Augustijns, P. Supersaturating drug delivery systems: The answer to solubility-limited oral bioavailability? *J. Pharm. Sci.* **2009**, *98*, 2549.